0026-895X/03/6306-1417–1429$7.00
MOLECULAR PHARMACOLOGY
Copyright © 2003 The American Society for Pharmacology and Experimental Therapeutics
Mol Pharmacol 63:1417–1429, 2003

Vol. 63, No. 6
2015/1067941
Printed in U.S.A.

Local Anesthetic Block of Kv Channels: Role of the S6 Helix and the S5-S6 Linker for Bupivacaine Action

JOHANNA NILSSON, MICHAEL MADEJA, and PETER ÅRHEM

The Nobel Institute for Neurophysiology, Department of Neuroscience, Karolinska Institutet, Stockholm, Sweden (J.N., P.Å.); and Institut für Physiologie, Münster, Germany (M.M.).

Received July 18, 2002; accepted March 10, 2003

This article is available online at http://molpharm.aspetjournals.org

ABSTRACT

To gain insights in the molecular mechanisms of anesthesia, we analyzed the effects of bupivacaine on a series of voltage-gated K^+ channels (Kv1.1, -1.2, -1.5, -2.1, -3.1, and -3.2) and various mutant channels derived from Kv2.1, using *Xenopus laevis* oocytes. Two phenomenologically different blocking effects were seen at room temperature: a time-dependent block of Kv1 and Kv3 channels (K_d between 110 and 240 μM), and a time-independent block on Kv2.1 (K_d = 220 μM). At 32°C, however, Kv2.1 also showed a time-dependent block. Swapping the S6 helix between Kv1.2 and Kv2.1 introduced Kv1.2 features in Kv2.1. Critical residues were located in the N-terminal end of S6, positions 395 and 398. The triple substitution of residues 372, 373, and 374 in the S5-S6 linker decreased the bupivacaine affinity by 5-fold (K_d increased from 220 to 1170 μM). The results suggest that bupivacaine blocks Kv channels by an open-state–dependent mechanism and that Kv2.1 deviates from the other channels in allowing a partial closure of the channel with bupivacaine bound. The results also suggest that the binding site is located in the internal vestibule and that residues in the descending P-loop and the upper part of S6 are critical for the binding, most likely by allosteric mechanisms. A simple mechanistic scenario that explains the observations is presented. Thermodynamic considerations suggest that the interaction between bupivacaine and the channels is hydrophobic.

Local anesthetics are important clinical tools, used in controlling pain, cardiac arrhythmias, and epileptic seizures. Although voltage-gated Na^+ channels are the main targets for local anesthetics, clinically important side effects may be produced by lower affinity block of voltage-gated K^+ channels. For instance, bupivacaine has been reported to induce lethal arrhythmias by affecting cardiac K^+ channels (Albright, 1979; Mather and Chang, 2001).

The blocking mechanism has been described as a complex state-dependent process in both Na^+ (Hille, 1977, 2001; Hondeghem and Katzung, 1977; Butterworth and Strichartz, 1990) and K^+ channels (Valenzuela et al., 1995), with binding preferentially in open or in inactivated channel states. Several binding sites have been proposed in both Na^+ (Hille, 2001) and K^+ channels (Longobardo et al., 2000), but the most extensively discussed hypothesis assumes a single site, located in the internal pore mouth (Lipka et al., 1998; Hille, 2001), early postulated to be delimited by the S6 helix and the P-loop. The importance of S6 for the binding has been confirmed for both Na^+ and K^+ channels (Ragsdale et al., 1994; Franqueza et al., 1997).

The molecular details of the blocking process are poorly known. The crystallization of the KcsA channel (Doyle et al., 1998), however, has opened up new possibilities to investigate these processes in K^+ channels, including molecular dynamics simulations (Åqvist and Luzhkov, 2000).

To prepare the ground for such attempts, and to better understand the clinical side effects mentioned above, we analyzed the effects of bupivacaine on a series of wild-type Kv channels (Kv1.1, -1.2, -1.5, -2.1, -3.1, and -3.2) expressed in *Xenopus* oocytes. Besides the reasons listed above, there are further advantages with using the mentioned set of K^+ channels. They have relatively slow and simple kinetics and do not show fast inactivation (making it possible to study the binding without complications caused by competition from the inactivation particle). They are structurally variable in the pore region, making our approach a natural site-directed mutagenesis. They also show differential sensitivity to general anesthetics (Harris et al., 2000).

The results showed that bupivacaine at room temperature causes a time-dependent block of the studied Kv1 and Kv3 channels, and a time-independent block on Kv2.1. However, a time-dependent effect on Kv2.1 was seen at 32°C. Analysis of the effects of replacing residues in Kv2.1 by corresponding Kv1.2 residues (Fig. 1, A and B) in the internal vestibule delimiting structures (the S6 helix and the S5-S6 linker), showed that N-terminal end substitutions in S6 introduced

This work was supported by Swedish Medical Research Council grant 6552, the Swedish Society of Medicine, the Swedish Society for Medical Research, the KI foundation, and Deutsche Forschungsgemeinschaft grant SFB556, A3.

ABBREVIATIONS: TEA, tetraethylammonium.

Kv1.2 features with respect to the bupivacaine block. P-loop substitutions decreased the affinity of bupivacaine 5-fold.

The results suggest that bupivacaine blocks Kv channels by an open-state–dependent mechanism. The data are consistent with a binding site located in the internal vestibule. Numerical simulations suggest that the effect on Kv2.1 deviates from that on the other channels in allowing a partial closure of the channel in bound state. The mutational experiments suggest that residues in the descending P-loop and the upper part of S6 are critical for the binding, most likely by an allosteric mechanism. A simple mechanistic scenario explaining the observations is presented. One crucial feature of this scenario is the small distances between the critical residues and the conserved glycine residue in the S6 helix recently shown to act as a gating hinge (Jiang et al., 2002; Yifrach and MacKinnon, 2002). Thermodynamic considerations suggest that the interaction between bupivacaine and the channels is hydrophobic.

Materials and Methods

Molecular Biology. cRNA for the rat Kv1.1, -1.2, -1.5, –3.1, and -3.2, and human Kv2.1 was synthesized by using the plasmid pAS18 as template for SP6 polymerase (Stühmer et al., 1988). The channel constructs used were all modified hKv2.1 channels (Swiss-Prot TrEMBL accession number Q14193), comprising introductions of rKv1.2 residues (Swiss-Prot accession number P15386). A lineup of the S5-S6 linker and the S6 segment of the used wild-type, chimeric, and point-mutated channels is shown in Fig. 1A.

For cRNA synthesis, the corresponding plasmid DNAs were linearized. The transcription reactions were performed using a com-

A

```
                          --------P-loop-------    -------------S6-------------
hKv2.1        353 EKDEDDTKFKSIPASFWWATITMTTVGYGDIYPKTLLGKIVGGLCCIAGVLVIALPIPIIVNNFSE
rKv1.2        350 -A--R-SQ-P---DA----VVS--------MV-T-IG-----S--A-----T----V-V--S--NY
rKv3.1        367 -R****-H--N--IG----VV----L----M-Q--WS-ML--A--L-----T--M---V-----GM
KcsA           51 ERGAPGAGLITY-RAL--SVE-A-------L-PV--W-RL-AVVVMV-ITSFGITVTAALATW-VG

ChS5-S6       353 -A--R-SQ-P---DA----VVS--------MV-T-IG------------------------------
MuS5-P        353 -A--R-SQ-P--------------------------------------------------------
MuP-S6        353 ----------------------------------T-IG------------------------------
MuS5-P/P-S6   353 -A--R-SQ-P------------------------T-IG------------------------------
Mu 366        353 -------------DA--------------------------------------------------
Mu 372        353 -------------------VVS-------------------------------------------
Mu 383        353 -------------------------------MV-----------------------------------

ChS6          353 ---------------------------------------S--A-----T----V-V--S--NY
Mu 395        353 ---------------------------------------S--A--------------------
Mu 404        353 ------------------------------------------------T---------------
Mu 409        353 ---------------------------------------------------V-V--S----
Mu 417        353 ------------------------------------------------------------NY

**** = IGAQPNDPSASEH
```

B

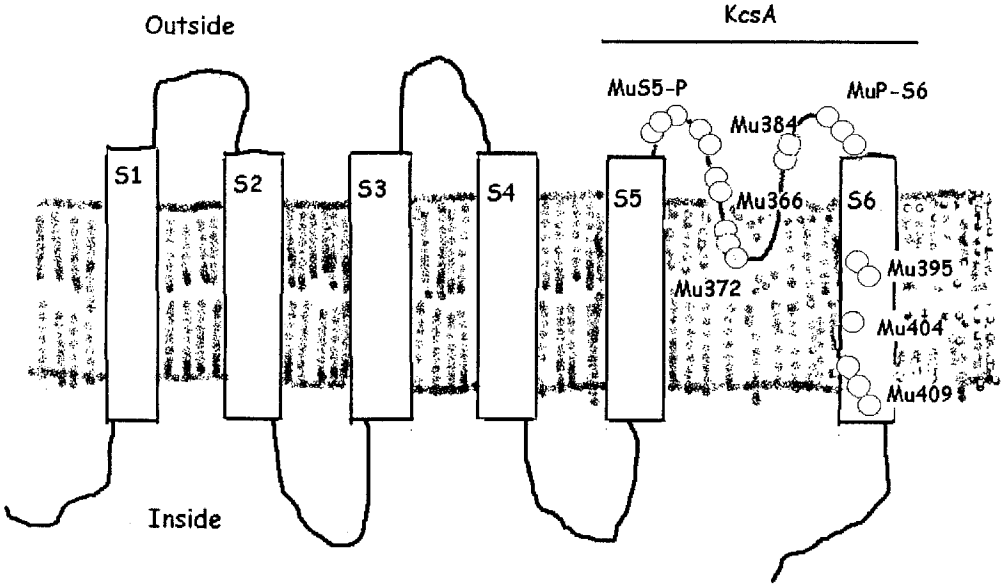

Fig. 1. A, sequence alignment of the S5-S6 linker and the S6 segment of rKv1.2, hKv2.1, rKv3.1, KcsA, and mutated hKv2.1 channels, respectively. The sequences shown are: hKv2.1, *Homo sapiens* (Swiss-Prot TrEMBL accession number Q14193); rKv1.2, *Rattus norvegicus* (Swiss-Prot accession number P15386); rKv3.1, *R. norvegicus* (Swiss-Prot accession number P25122); and KcsA *Streptomyces lividans* (PIR accession number S60172). B, schematic diagram of the transmembrane topology of a Kv subunit with location of the substitutions indicated. The region corresponding to the KcsA channel (the pore region) is marked.

mercial kit (mMessage mMachine; Ambion, Austin, TX) and T7 RNA polymerase. Oocytes of the South African clawed toad (*Xenopus laevis*) were used as expression system. Oocytes in stage V or VI were isolated manually from the ovary and injected with the cRNA dissolved in distilled water at a concentration of 0.5 ng/oocyte (non-Kv2.1 channels) or 0.01 ng/oocyte (Kv2.1). The injected oocytes were maintained at 20°C until used for experiments. The electrophysiological experiments were performed 3 to 5 days after injection of cRNA.

Electrophysiology. The investigations were performed with a two-electrode voltage-clamp technique, modified to include a concentration-clamp technique (Madeja et al., 1991). The pipettes used were of borosilicate glass (Hilgenberg, Malsfeld, Germany) with a resistance of 0.5 to 1 MΩ when filled with 3 M KCl. Data acquisition and analysis were made with pCLAMP software (Axon Instruments, Union City, CA). The holding potential was −80 mV and currents associated with steps in increments of 10 to +60 mV were recorded before and after application of bupivacaine in various concentrations (see below).

A high cRNA concentration was used for injection to obtain a high channel density. The consequent series resistance problem was avoided by making the critical measurements at relatively low currents. The volume resistance of the external solution between membrane and ground was estimated to be between 0.1 and 1 kΩ. The resulting voltage error in measurements of midpoint values and of blocking time courses was estimated to be less than 1 mV. The relatively long settling time of the potential steps (partly because of the large membrane capacitance; Finkel and Gage, 1985) clearly depended on the size of the current. The resulting error was negligible at currents below 5 μA and, consequently, in the measurements at the used bupivacaine concentrations. However, it affected the control currents at high potential steps. We therefore discarded the first 2 ms of these recordings in the quantitative analysis. The results are given as mean ± S.D.

Solutions. The tissue culture solution was a modified Barth medium (88 mM NaCl, 1 mM KCl, 1.5 mM $CaCl_2$, 2.4 mM $NaHCO_3$, 0.8 mM $MgSO_2$, and 5 mM HEPES, pH 7.4, which was supplemented with penicillin (100 IU/ml) and streptomycin (100 μg/ml). The electrophysiological experiments were made with two types of solution, normal Ringer's solution and high [K^+] solution. The latter type was used for investigating tail currents. The composition of the control Ringer's solution was 115 mM NaCl, 2 mM KCl, 1.8 mM $CaCl_2$, and 10 mM HEPES, pH 7.2. The composition of the control high [K^+] solution was 2.5 mM NaCl, 120 mM KCl, 1.8 mM $CaCl_2$, and 10 mM HEPES, pH 7.2. The test solutions consisted of bupivacaine (Sigma Chemical Co, St. Louis), added to the control solutions in concentrations of 30, 100, 300, and 1000 μM.

To investigate the possibility of external binding sites, bupivacaine was in some experiments replaced by the permanently charged analogs LEA-113 (bupivacaine analog), LEA-120 (lidocaine analog), and RAD-250 (mepivacaine analog) in concentrations up to 1000 μM. The analogs were gifts from Astra (Södertälje, Sweden).

Data Analysis. The time course of the block was quantified by fitting a sum of two exponentials to the current recordings in the time window 2 to 500 ms with a nonlinear correlation procedure (Chebyshev method; pCLAMP software, Axon Instruments).

The steady state K^+ conductance $g(V)$ was calculated as

$$g(V) = I(V)/(V - E_K) \quad (1)$$

where $I(V)$ is the steady-state current, V is the absolute membrane potential, and E_K is the equilibrium potential (assumed to be −80 mV).

The dose-response curves were fitted to the equation

$$y = 1/(1 + (c/K_d(V)^{n_H} \quad (2)$$

where y represents either normalized steady-state current [$I(t)$], normalized steady-state conductance [$g(t)$], or normalized steady-state open probability [$P_o(t)$] at potential V (usually +60 mV). c denotes bupivacaine concentration, n_H is the Hill coefficient, and $K_d(V)$ is the dissociation constant of the reaction at potential V.

Kinetic and Structural Model Simulations. To describe the experimental results, we used the kinetic schemes described under *Results*. They were solved numerically and fitted to the experimental data. Scheme 1 will briefly be discussed below. The extended version, Scheme 2, was solved correspondingly. Scheme 1 is described by the following system of differential equations:

$$\begin{aligned} dP_1(t)/dt &= -\alpha P_1 + \beta P_2 \\ dP_2(t)/dt &= \alpha P_1 - (\beta + \kappa c) P_2 + \lambda P_3 \\ dP_3(t)/dt &= \kappa c P_2 - \lambda P_3 \end{aligned} \quad (3)$$

where P_1, P_2, and P_3 are the probabilities that the system is in states C, O, and B, respectively at time t. The initial condition was chosen such that the system is in state C ($P_1 = 1$) at time 0. The rate constants of the activation were

$$\alpha = k_{eq} \exp(q0.5(V - V_0)F/RT) \quad (4)$$

$$\beta = k_{eq}\exp(q0.5(V_0 - V)F/RT)$$

where V is the absolute membrane potential, F is the Faraday constant, R is the real gas constant, T is the absolute temperature, the rate constant at $V = V_0$, and q is the valence of the transition. The voltage dependence of the blocking transition was assumed to be described by the factor $\exp(-\delta V F/R T)$ multiplied with the unblocking rate constant λ. δ is the fraction of the field sensed by the charged bupivacaine molecule in its blocking action (the electrical distance).

Eq. 3 was solved by a simple Euler integration method. The time interval used was 10 μs. For the cases (Kv1.1, -1.2, and -3.2) in which the $g(V)$ curves showed a clear saturation level within the investigated voltage range (<+60 mV), the electrical distance δ could be directly estimated from the $g(V)$ curve by fitting the experimental data to the following equation:

$$g(V)/g_{ctrl}(V) = 1/[1 + c \exp(\delta VF/RT)/K_d(0)] \quad (5)$$

where $g_{ctrl}(V)$ is the conductance in control solution and $K_d(0)$ is the dissociation constant at $V = 0$ mV. The structural model simulations of the mutated channels were performed with SwissPdb Viewer (version 3.7).

Results

Analysis of Wild-Type Channels

Two Types of Effect. Figure 2A shows the effect of 0, 100, 300, and 1000 μM bupivacaine on currents associated with a test step to +60 mV for all the wild-type channels studied. Except for the case of the Kv2.1 channel, the effect is a time-dependent reduction. For the Kv2.1 channel, no such time dependence is evident, suggesting a deviating blocking mechanism. However, this channel also deviates from all the other channels in showing a considerably slower activation time course. The time to half maximum current value ($t_{1/2}$) at +60 mV varied between 3.7 and 6.2 ms for Kv1 and 3 channels, whereas it was 12 ms for Kv2.1. Mean values are listed in Table 1. The slower activation of the Kv2.1 channel will have consequences for the interpretation of the bupivacaine effect on Kv2.1 as will be described below.

Figure 3 shows the concentration dependence of the steady-state reduction for each channel investigated, measured at +60 mV and 500 ms. Each data point represents mean values from 4 to 12 cells. Fitting Eq. 2 to the data gives

dissociation constants in the range 110 to 240 μM and Hill coefficients in the range 1.0 to 1.4 for the different channel types, suggesting 1:1 reversible reactions between bupivacaine and the channel protein (see Table 1).

Time-Dependent Effects Suggest an Open-State–Dependent Mechanism. The time-dependent current reduction evident in the non-Kv2.1 channels suggests that a considerable fraction of the bupivacaine molecules binds to the

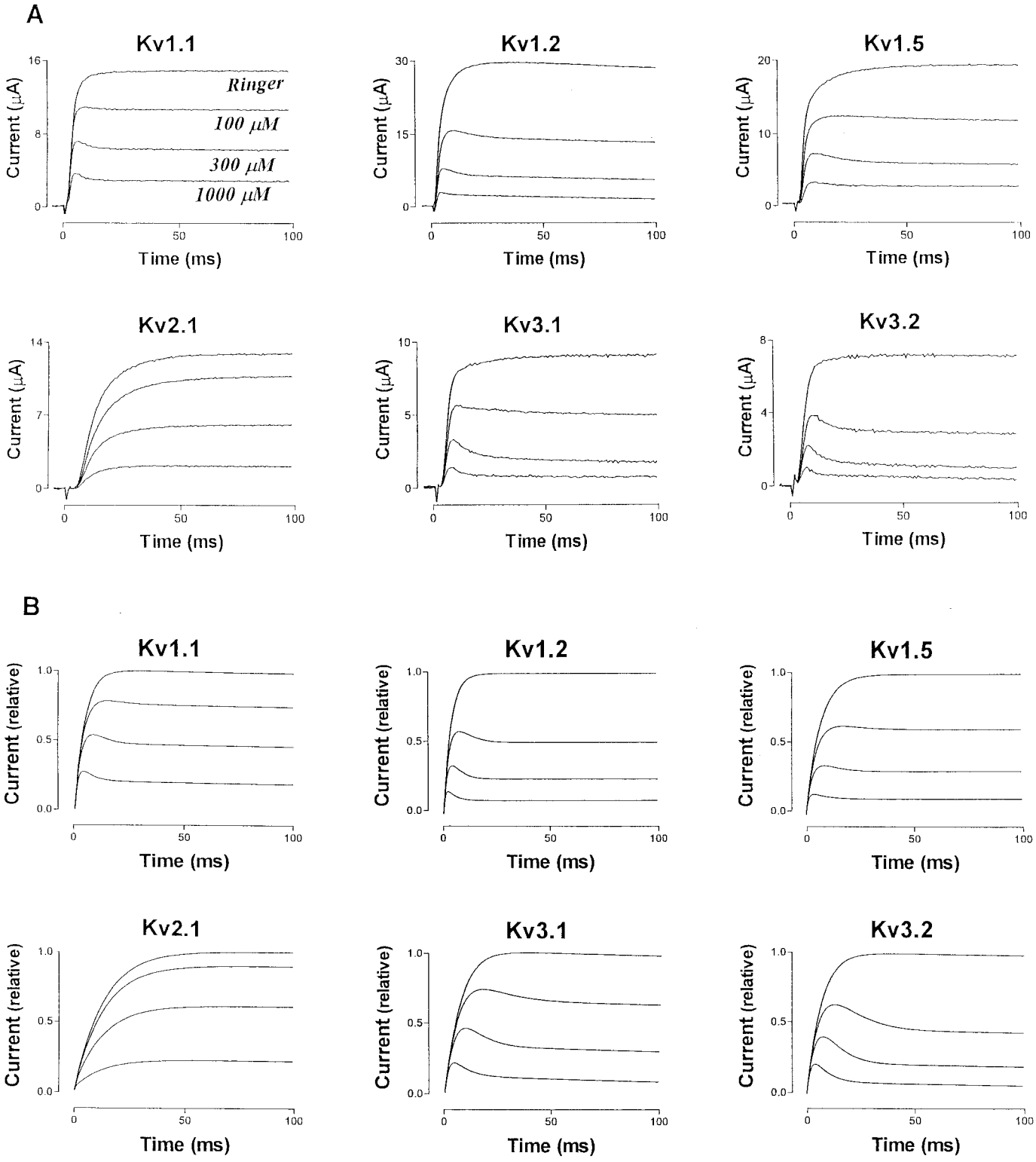

Fig. 2. The effect of bupivacaine (0, 100, 300, and 1000 μM) on the ionic currents of Kv channels indicated. Step potential +60 mV and holding potential −80 mV. Control in Ringer's solution. A, experimental data. B, computer simulation of Scheme 1 fitted to the data in Fig. 2A. Resulting $K_d(60)$ (millimolar), α (per millisecond) and κ (millisecond/millimolar) values are: Kv1.1, 0.25, 0.23, 0.5; Kv1.2, 0.10, 0.27, 1.2; Kv1.5, 0.12, 0.15, 0.7; Kv2.1, 0.25, 0.08, 1.8; Kv3.1, 0.12, 0.16, 0.5; Kv3.2,0.080, 0.17, 0.5.

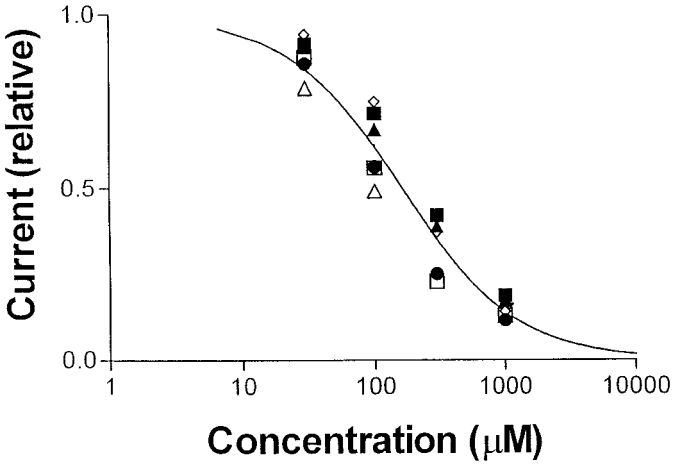

Fig. 3. Dose-response curve for steady-state block of the channels studied. ■, Kv1.1; ▲, Kv2.2; ●, Kv1.5; ◇, Kv2.1; □, Kv3.1; △, Kv3.2. Continuous line is the solution of Eq. 2 fitted to the mean steady-state block (n = 4–12 for each channel). K_d = 160 μM and n_H = 1.1. Mean K_d values for each channel are given in Table 1.

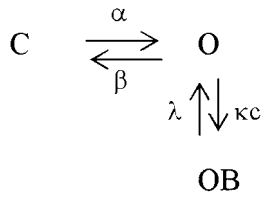

Scheme 1. C, O, and OB denote closed, open, and blocked states, respectively; α and β are activation and deactivation rate constants, respectively; κ and λ are binding and unbinding rate constants, respectively; and c is the bupivacaine concentration.

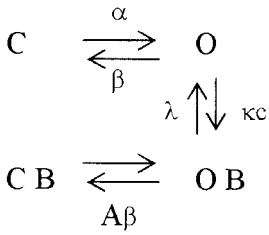

Scheme 2. A is a constant (<1) reflecting a decreased rate of closing in bound state.

channel preferentially when it is open. To determine whether such a mechanism could fully describe the block, we used a simple kinetic scheme (Scheme 1). The scheme can easily be extended to include several closed states to better fit the experimentally observed activation phase. However, the experimental resolution of this phase was limited because of the frequency response of the amplifier system (see *Materials and Methods*), and we found it sufficient for the present purpose to use the simpler Scheme 1.

Time Course Analysis. We thus fitted Scheme 1 (by fitting numerical solutions of Eq. 3) simultaneously to the experimental data (current time courses) at 0, 100, 300, and 1000 μM bupivacaine for the different channels in Fig. 2A, using the $K_d(60)$ values listed in Table 1. The resulting curves of this global fit procedure are shown in Fig. 2B. The values of activation and blocking/unblocking rate constants (α, κ, and λ respectively) are given in the figure legend. The good fit between the experimental data and the calculated curves suggest that the block can be described by Scheme 1 type kinetics. However, because the block of Kv2.1 did not display a peaked time course, it was not possible to uniquely determine the blocking rate constants but only minimum values. This means that, at this stage, we cannot exclude the idea that other blocking mechanisms, comprising a state-independent component, explain the experimental observations.

The cause of the nonpeaked time course in Kv2.1 channel might be the slow activation time (compared with the other Kv channels), masking a time-dependent blocking time course. We tried to clarify this issue by increasing the activation rate. There are two easy ways to experimentally accomplish this: to increase the temperature (compared with the previously used room temperature) and to increase the potential (compared with the previously used highest potential +60 mV). We used both ways. Figure 4 shows the results from an experiment, in which the temperature was increased from 24 to 32°C. The rate of activation increased 3-fold (mean $t_{1/2}$ is decreased from 12 ± 1 to 4.0 ± 0.2 ms; n = 3) and a time dependence of the bupivacaine block (300 μM) at 32°C was clearly evident. Similar results were obtained in experiments with test steps up to +100 mV. The rate of activation was increased 45% (mean $t_{1/2}$ is decreased from 12 ± 1 ms to 8.3 ± 0.6 ms; n = 5), and a time dependence of the block of 300 μM was visible (data not shown).

Both types of experiments suggest that the block of Kv2.1 comprises an open-state dependent component. However, Scheme 1 was too simple to fully explain the block. We therefore extended it by assuming that the channel partially closes in bound state according to Scheme 2. When A was assumed to be 0.4, this scheme better explained the block of Kv2.1 channels than Scheme 1 where A = 0. However, it was difficult to obtain good estimations of the blocking time constant, and thus of the constant A, from the time course measurements because of poor experimental resolution (no

TABLE 1
Mean dissociation constant (K_d) at +60 mV for the different K channels investigated
Also shown are time to half-maximal current at +60 mV ($t_{1/2}$), midpoint value of the conductance versus voltage curve ($V_{1/2}$) in control solution, and Hill coefficients (n_H).

Channel Type	n	$t_{1/2}$	$V_{1/2}$	$K_d(60)$	n_H
		ms	*mV*	*μM*	
Kv1.1	4	4.4 ± 0.2	−29 ± 2.4	240 ± 20	1.1 ± 0.3
Kv1.2	12	3.7 ± 0.3	−13 ± 0.9	210 ± 20	1.1 ± 0.1
Kv1.5	6	4.9 ± 0.3	+5 ± 2.1	130 ± 35	1.2 ± 0.1
Kv2.1	10	12.0 ± 1.0	+7 ± 0.9	220 ± 30	1.4 ± 0.1
Kv3.1	4	6.2 ± 1	+18 ± 2.1	130 ± 30	1.3 ± 0.2
Kv3.2	5	5.2 ± 0.6	+6 ± 2.4	110 ± 20	1.0 ± 0.2

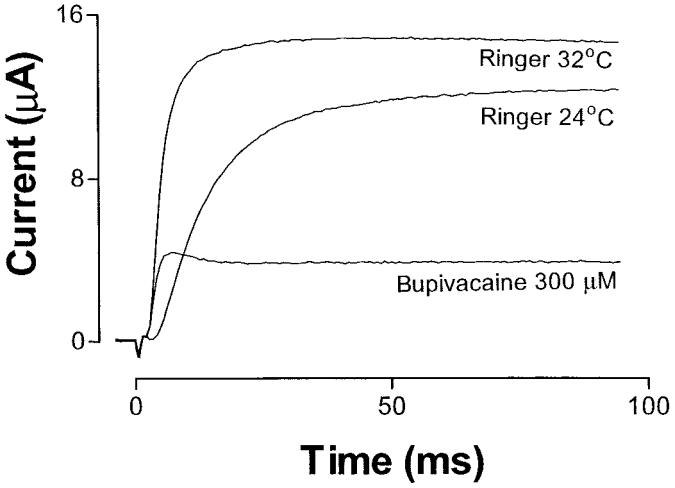

Fig. 4. Effect of increased activation rate on block of Kv2.1 by a temperature increase from 24 to 32°C. Bupivacaine concentration, 300 μM. Note the time dependence of block. For comparison, control curves in Ringer's solution at 24 and 32°C are shown. Test step, +60 mV; holding potential, −80 mV.

pronounced peak). We therefore estimated A from the steady-state $g(V)$ curves, which proved to be a more reliable method.

Steady-State Conductance Curve Analysis. We thus calculated steady state $g(V)$ curves for different bupivacaine concentrations and fitted numerical solutions of Scheme 2 to the data. The voltage dependence of the activation and blocking/unblocking transition was assumed to follow equations as described under *Materials and Methods* (Eq. 4 and associated formulas). Fitting Scheme 2 simultaneously to data for 0, 100, 300, and 1000 μM yielded values of the activation rate constants α and β, the blocking rate constants κ and λ, the constant A, and the electrical distance δ.

The experimental results confirmed and extended the observations from previous studies (Elinder et al., 1996) on the variability of activation range for the different channels. The midpoints ($V_{1/2}$) in control solution were found to range from −29 mV (for Kv1.1) to +18 mV (for Kv3.1) and are listed in Table 1. The results also confirmed that the block of Kv2.1 deviated from that of the other channels. For all the non-Kv2.1, the block could be described by Scheme 2 with A = 0 (i.e., Scheme 1), whereas for Kv2.1, A = 0.44 ± 0.06 (n = 4).

The difference between the block of Kv2.1 and of the other channels is illustrated in Fig. 5; A shows the effect of 300 μM bupivacaine on the $g(V)$ curve of Kv1.5 and B shows the effect on the $g(V)$ curve of Kv2.1 in comparison with solutions of Scheme 2, assuming $A = 0$ and $A = 1$. The experimental $g(V)$ curve for Kv1.5 closely follows the curve predicted by $A = 0$ (no closure), whereas that for Kv2.1 is situated between the solutions for $A = 0$ and $A = 1$.

The block was slightly voltage dependent. The fitting procedure described above (simultaneous fitting of Scheme 2 to measurements in different bupivacaine concentrations) yielded values of the electrical distance of the binding site for the different channels. The values varied between 0.10 and 0.25 (n = 4–6 for each channel). A more direct estimation of the electrical distance was also possible for channels from which several $g(V)$ points at fully activated channels were available. Kv1.1, -1.2, and -3.2 belonged to this category, and the electrical distances for these channels, obtained from fitting Eq. 5 to the experimental points, were 0.17 ± 0.02, 0.13 ± 0.03, and 0.18 ± 0.01, respectively (n = 4 for each channel), near the values obtained from the more complete fitting procedures described above (fitting Scheme 2).

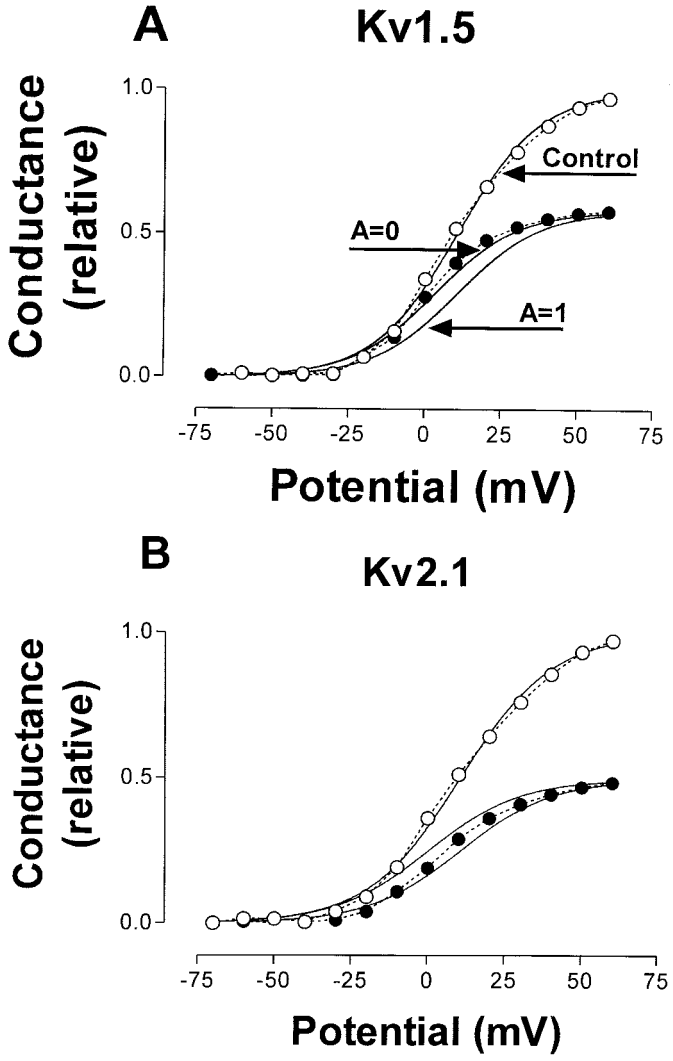

Fig. 5. Effects of 100 and 300 μM bupivacaine, respectively, on $g(V)$ curves for Kv1.5 (A) and Kv2.1 (B). Continuous lines are computer simulations of steady-state open probability curves for Scheme 2, assuming K_d values according to Table 1. The left curve is a simulation of Scheme 4 with $A = 0$ and the right curve with $A = 1$. Interrupted lines connect the experimental points.

In summary, the simulations and fitting procedures applied to the steady state $g(V)$ curves show that the bupivacaine block of the Kv channels studied can all be explained by a simple open-state–dependent mechanism, described by the unitary Scheme 2. What differs between the block of the different channels is the degree of closure at repolarization (i.e., the value of the constant A). Kv2.1 channels can partially close (A = 0.4), whereas Kv1 and -3 channels cannot (A = 0). The small electrical distances obtained suggest that the binding sites in all studied channels are located superficially (in electrical terms) on the internal side.

Tail Current Experiments Support the Partial Closure Hypothesis. The $g(V)$ curve analysis above of the bupivacaine effect on the closing transition in bound state was supplemented by an analysis of the effects on tail currents in high [K^+] solutions. This approach allows a direct estimation

of the bupivacaine effect on the rate of the backward transition (OB→CB) and thus of factor *A*. Figure 6A shows tail currents at −80 mV computed from Scheme 2 for the cases $A = 0$ and $A = 0.4$. The difference between the crossing-over points of the test-control curves in the two cases is clear. Figure 6, B and C, shows the effect of 300 μM bupivacaine on the tail current associated with a step from +60 to −80 mV in high $[K^+]$ solutions for Kv2.1 and Kv1.2, as representative for the non-Kv2.1 channels. A comparison between the experimental and the simulation curves suggests, in agreement with the conclusions above, that the bupivacaine effect on Kv1.2 is well explained by a nonclosure mechanism ($A = 0$) and that on Kv2.1 by a partial closure mechanism ($A = 0.4$). This in turn strengthens the view that bupivacaine affects the gating mechanisms in Kv2.1 and Kv1.2 (and thus the non-Kv2.1 channels) in quantitatively different ways, suggesting structural differences.

The increased external $[K^+]$ in the tail experiments affected the blocking kinetics of bupivacaine. Fitting Scheme 2 to the experimental curves for Kv2.1 and Kv1.2 gave κ and λ values that were, compared with the values in Ringer test solutions, reduced by 3- to 5- and 2-fold, respectively, yielding a slight K_d increase (about 50%). The effect was, unexpectedly, voltage-independent, being equal at both +60 and −80 mV, and thus independent of the current direction through the pore. This suggests an interaction between external K^+ and the bupivacaine binding site, most likely by an allosteric mechanism (see *Discussion* for the location of the binding site).

No Effect by Permanently Charged Local Anesthetics. In conclusion, the results suggest a single-site blocking mechanism for all channels studied. This conclusion was supported by results from experiments on Kv2.1 and Kv1.2 with permanently charged local anesthetic analogs, assumed to act exclusively from the external side. We used the bupivacaine analog LEA-113, the lidocaine analog LEA-120, and the mepivacaine analog RAD-250. They were applied in concentrations of up to 1000 μM for 10 min. No effect was observed for any analog on either of the two channels: LEA-113 was tested on six oocytes, RAD-250 on eight oocytes, and LEA-120 on four oocytes (data not shown).

Mutational Analysis

Substituting the S6 Helix Impairs Channel Closing in Bound State. The S6 helix is expected to play a role for the binding of local anesthetics (Ragsdale et al., 1994; Franqueza et al., 1997). It is also assumed to be directly involved in the gating process (Yellen, 1998; Scholle et al., 2000). There are, therefore, at least two reasons to expect modifications of the bupivacaine effect on Kv2.1 after a Kv1.2 S6 helix substitution: an indirect effect caused by increased activation rate, causing a visible time-dependent block, and a direct effect caused by structural modifications in the binding region, decreasing the probability of closing the channel in bound state.

The effect of the S6 helix substitution per se is demonstrated in Fig. 7. The rate of activation is faster [$t_{1/2}$(60) is 7.7 versus 12 ms; see Table 2] and the $g(V)$ curve is strongly shifted to the left compared with that of the wild type ($V_{1/2}$ shift is −36 mV; see Table 2). Compared with the donor channel (Kv1.2), however, the chimera does not activate as fast ($t_{1/2}$ at +60 mV is 7.7 versus 3.7 ms), but it activates at more negative potentials ($V_{1/2}$ shift is −14 mV).

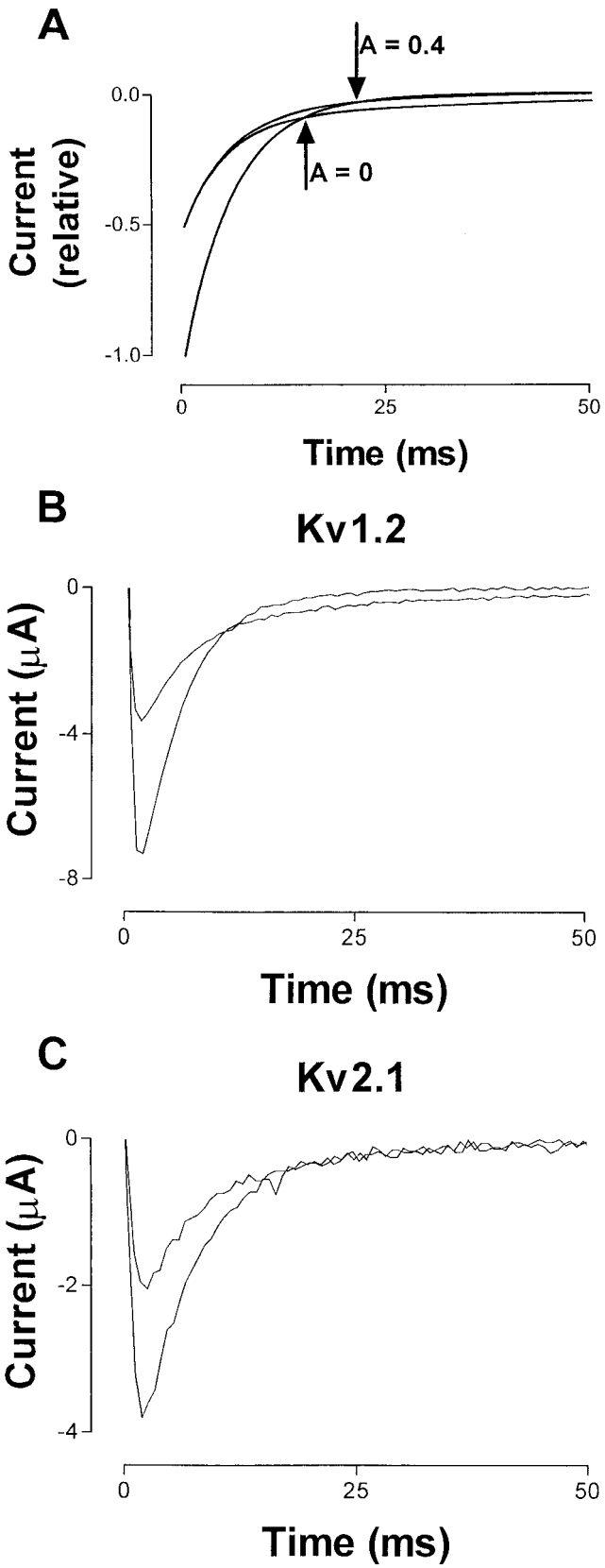

Fig. 6. Effects of bupivacaine on tail currents. *A*, simulation of Scheme 4 with $A = 0$, $A = 1$, and $A = 0.4$. Note the crossing-over (arrows). B and C, effects of 300 μM bupivacaine on tail currents, associated with a step to −80 mV from +60 mV for Kv1.2 and Kv2.1 Measurements were made in high $[K^+]$ solutions. Note the close resemblance between the Kv2.1 case and the simulation of the $A = 0.4$ case in A.

Thus, the effect of bupivacaine on the S6 substituted chimera ChS6 was, as expected, time dependent (Fig. 7A). This lends support to the conclusion that Kv2.1 comprises an open-state–dependent site for bupivacaine, normally masked by a slow activation. Furthermore, analyzing the $g(V)$ curve (Fig. 7B) by fitting Scheme 2 to the experimental data suggests that the channel probability of closing in bound state is very small in the S6 substituted chimera; i.e., its kinetics is explainable in terms of the scheme with $A = 0$. In summary, introducing the S6 helix of Kv1.2 into Kv2.1 induces Kv1.2 behavior with respect to bupivacaine action. The same conclusion is suggested by the change in the A value, reflecting the resistance to closing with bupivacaine bound at repolarization (0.03 versus 0.44; Table 1). The K_d value of the steady-state block at +60 mV is about 2-fold higher for ChS6 than that of wild-type Kv2.1 (520 versus 220 μM; Table 2).

N-terminal End Residues Are Critical for the Impaired Closing. To analyze the role of the specific residues

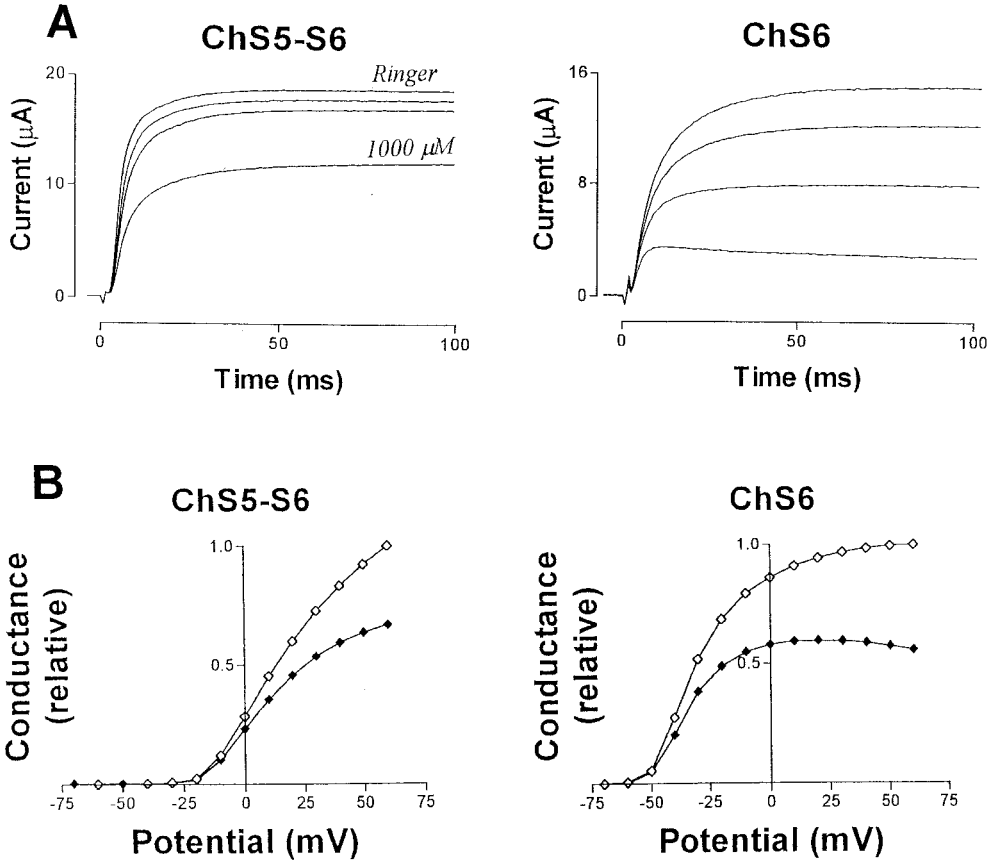

Fig. 7. Effects of bupivacaine on the S5-S6 linker (ChS5-S6) and the S6 helix (ChS6) chimeras. Control curves from Ringer's solution measurements. A, current time course for a test pulse to +60 mV from a holding potential of −80 mV. The bupivacaine concentrations are 0, 100, 300, and 1000 μM. B, conductance versus voltage curves (Eq. 1). The bupivacaine concentration is chosen to block about 50% at +60 mV. ChS5-S6, 1 mM; ChS6, 300 μM.

TABLE 2

Dissociation constants (K_d) for the different K^+ channels investigated (Eq. 2)

$V_{1/2}$ is the midpoint of the $g(V)$ curve (Eq. 1) and $\Delta V_{1/2}$ is the difference relative the midpoint value for Kv2.1. $t_{1/2}$ is the time to half-maximal current at + 60 mV. A value reflects the propensity of channel closing in bound state.

Channel	n	$V_{1/2}$	$\Delta V_{1/2}$	$t_{1/2}$	K_d	A
		mV	*mV*	*ms*	μM	
Kv2.1	10	+7 ± 0.9	±0	12.0 ± 1	220 ± 30	0.44 ± 0.07
Kv1.2	12	−13 ± 0.9	−22	3.7 ± 0.3	210 ± 20	0.00 ± 0.07
S6 Modifications						
ChS6	5	−29 ± 2	−36	7.7 ± 0.4	520 ± 50	0.03 ± 0.08
Mu395	5	+6 ± 4	−1	6.6 ± 0.4	220 ± 50	0.05 ± 0.05
Mu404	5	+11 ± 6	+4	5.1 ± 0.2	420 ± 40	0.51 ± 0.10
Mu409	5	+16 ± 1	+9	6.1 ± 0.6	330 ± 60	0.47 ± 0.07
Mu417	6	−4 ± 2	−1	11.4 ± 0.7	170 ± 20	0.56 ± 0.08
S5-S6 Linker Modifications						
ChS5-S6	5	+14 ± 1	+7	7.9 ± 1.1	1150 ± 60	0.35 ± 0.07
External Residues						
MuS5-P	5	+8 ± 3	+1	11.7 ± 1.6	180 ± 50	0.52 ± 0.10
MuP-S6	4	+2 ± 3	−5	7.2 ± 2.0	500 ± 40	0.52 ± 0.09
MuS5-P/P-S6	5	+8 ± 1	+1	9.4 ± 0.7	360 ± 50	0.45 ± 0.08
Pore-loop Residues						
Mu366	3	+3 ± 0.5	+4	7.2 ± 0.8	640 ± 40	0.50 ± 0.06
Mu372	6	+12 ± 2	+5	10.5 ± 1.4	1170 ± 30	0.46 ± 0.09
Mu383	3	+5 ± 1	−2	15.1 ± 2.1	330 ± 40	0.28 ± 0.05

in S6 important for the modified closing probability discussed above, we substituted smaller segments and single residues from Kv1.2 to Kv2.1 (Fig. 1). We used the channel constructs Mu395, Mu404, Mu409, and Mu417, which comprise substitutions of all the differing residues of the Kv2.1 and Kv1.2 S6 segments, for the experiments (see *Materials and Methods*). Except for Mu417, all the constructs showed a 2-fold increase in rate of activation compared with that of wild-type Kv2.1 ($t_{1/2}$ = 5.1–6.6 ms versus 12 ms; Table 2). As mentioned above, the corresponding increase for the whole S6 substitution was also 2-fold ($t_{1/2}$ = 7.7 ms; Table 2), suggesting a complex interaction between the residues involved in the activation process. Corresponding $g(V)$ curves showed relatively small deviations (but in different directions) from that of the wild-type Kv2.1 [i.e., in contrast to the S6-substituted chimera ($V_{1/2}$ shifts between +9 and −1 mV versus −36 mV; Table 2). In addition, the results here point to a complex, nonadditive interaction between the residues in determining the voltage dependence.

The effects of bupivacaine on the S6-modified channels are summarized in Table 2. A time-dependent block is evident at 1000 μM for all S6-modified channels (data not shown), supporting the hypothesis of an open-state–dependent mechanism, explaining the bupivacaine effect on Kv2.1. The K_d values for the S6-modified channels varied between 170 and 420 μM.

Analyzing the $g(V)$ curves by fitting Scheme 2 to the experimental data, we found that the bupivacaine effect on Mu395 was explainable in terms of the scheme with $A = 0$ (i.e., an open-state dependent mechanism with a very small probability to close with bupivacaine bound). In summary, introducing the 395 and 398 residues of Kv1.2 into Kv2.1 induces Kv1.2 behavior in Kv2.1 with respect to bupivacaine action. For Mu404, Mu409, and Mu417, the fitting procedures showed in all cases that $A > 0.4$ (Table 2); i.e., they are explained by an open-state–dependent mechanism similar to that of wild-type Kv2.1. Thus, they partially close with bupivacaine bound.

The effect of bupivacine on the closing transition is most easily investigated by analyzing the tail currents in high [K^+] solutions. As shown above, the tail current in the case of no closure in bound state (i.e., $A = 0$) is predicted to clearly cross over the corresponding current in control solution, whereas in the case of normal closure with bupivacaine bound (i.e., A = 0.4), the crossing-over is much less conspicuous (see Fig. 6A).

Figure 8 shows the effect of 300 μM bupivacaine on the tail current associated with a step from 60 to −80 mV in high [K^+] solutions for the chimeras Mu395, Mu404, and Mu409. In agreement with the conclusions above, a clear crossing-over is noted for Mu395, whereas the crossing-over for Mu404 and -409 is much less conspicuous.

In summary, the results suggest that introducing Kv1.2 residues in the N-terminal end of the S6 helix above the assumed gating region (i.e., the S6 helices crossing point at the level of Ile409, Ile411, and Asn414) modifies the bupivacaine block of Kv2.1 indirectly as well as directly; indirectly by unmasking an open-state dependent mechanism through an increased rate of gating (residues Gly395, Cys398, Val404, Ile409, Ile411, and Asn414) and directly by modifying the gating process, reducing the probability of closing in bound state (G395 and C398). The affinity of the binding site, however, was not affected by any of these substitutions. This deviates from the effect of the C-terminal double mutation S417N/E418Y, which slightly increased the affinity (Table 2).

The results highlight the importance of the S6 helix for the activation of gating; except for Mu417, all S6 constructs studied increase the activation rate (Table 2). The $g(V)$ curves are affected in a less homogenous way; a whole segment substitution causes a large negative shift whereas single residue substitutions cause relatively small shifts in both directions. As pointed out above, this implies that that the different residues interact in a complex way to open the activation gate.

Substituting the S5-S6 Linker Decreases the Affinity of Bupivacaine Binding. Part of the internal vestibule wall is formed by the P-loop and has been shown to be involved in the internal binding of TEA (Yellen et al., 1991). Thus, substituting the whole linker S5-S6 can be expected to be involved in bupivacaine binding. Furthermore, it is expected to give information on possible external binding sites.

The result of the S5-S6 substitution per se was found to be an increased rate of activation (Table 2). The mean time to half-maximal current at +60 mV ($t_{1/2}$) decreased from 12 to 7.9 ms. The $g(V)$ curve was slightly shifted in positive direction (mean, +7 mV).

The effect of the substitution on the bupivacaine action is shown in Fig. 7A. It shows the result of applying three concentrations of bupivacaine on ChS5-S6 at +60 mV. The main result is that the block is reduced compared with that of both Kv1.2 and -2.1. The mean K_d of blocking ChS5-S6 at +60 mV is 1150 μM compared with 220 μM for Kv2.1 and 210 μM for Kv1.2 (Table 2). The A value, however, is relatively little changed compared with that of Kv2.1 (0.35 versus

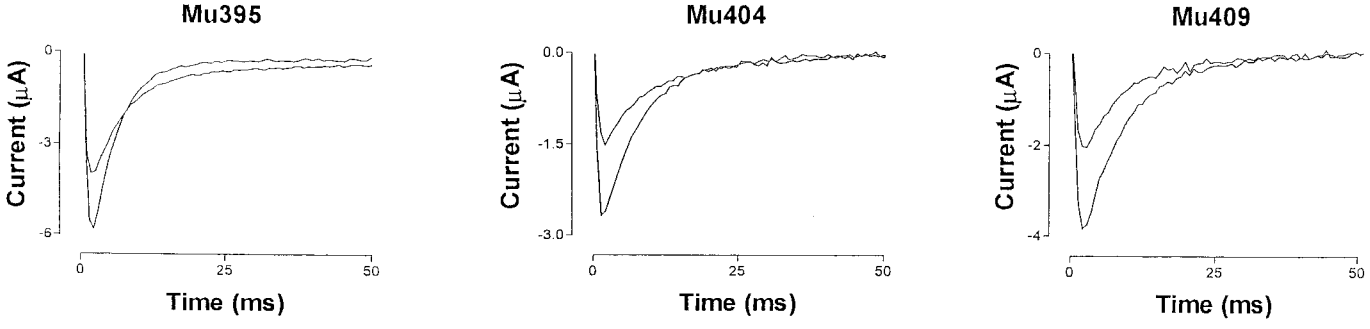

Fig. 8. Effects of 300 μM bupivacaine on tail currents, associated with a step to −80 mV from +60 mV for the mutated channels Mu395, Mu404, and Mu409. Note the clear crossing-over between control and bupivacaine currents for Mu395.

0.44; see Table 2), suggesting that the S5-S6 linker is functionally associated with the binding transition but not with the closing transition (i.e., it does not determine factor *A*).

External Vestibule Residue Substitutions Do Not Contribute to the Whole Linker Effect. The lower affinity induced by the S5-S6 linker substitution was unexpected. To identify the critical residues, we performed segment and single-residue substitutions (Fig. 1). The role of the external vestibule residues was analyzed by substituting the S5-P and P-S6 segments separately (ChS5-P and ChP-S6) and in combination (ChS5-P/P-S6). The role of the P-region was analyzed in more detail by using the following three constructs: Mu366, characterized by the double substitution A366D/S367A, Mu372, characterized by the triple substitution T372V/I373V/T374S, and Mu383, characterized by the double substitution I383M/Y384V (see Fig. 1).

The effects of the substitutions per se on time course and $g(V)$ curve are listed in Table 2. Effects ranged from negligible to increased rates of activation. Summarizing the results for the external vestibule residue substitutions, the increased rate of activation for the whole linker substitution is explained by residues in the P-S6 segment (mean $t_{1/2}$ at +60 mV decreased from 12 to 7.2 ms). This may be related to the reported evidence for an S6 involvement in gating. The midpoint of the $g(V)$ curve was only marginally affected. The affinity was considerably less affected by the external vestibule residues substitution than by the whole linker substitution (Table 2), confirming the conclusion from the results with permanently charged local anesthetics (see *Materials and Methods*) that no major block is exerted from binding to external residues. A slight time dependence of the block (i.e., the time course shows a peaked appearance) at 1000 μM was detected for the chimeras with increased rate of activation (ChS5-P/P-S6, ChP-S6), confirming the open-state–dependent blocking mechanism.

The analysis of the $g(V)$ curves confirms the results from the whole linker substitution; the S5-S6 linker is not functionally associated with the closing transition. This is reflected in the *A* values obtained [in the range 0.45 to 0.52 (Table 2)].

P-Loop Residues Are Critical for the Decreased Affinity. The P-loop residue substitutions resulted in more marked modifications of the block than the external residue substitutions. The effects of the substitutions per se are listed in Table 2. An increased rate of activation was noted for the substitutions in the N-terminal end of the P-loop (positions 366 and 367 in Kv2.1); the mean $t_{1/2}$ at +60 mV was decreased from 12 to 7.2 ms. The shifts of the $g(V)$ curves were small, the extremes being −2 and +5 mV.

The bupivacaine block was decreased by the triple-mutation T372V/I373V/T374S; the mean K_d value at +60 mV was increased to 1170 from 220 μM (Table 2). This suggests that the reduced affinity caused by the S5-S6 linker substitution is explained by modifications of the three-residue segment Thr372-Ile373-Thr374. In addition, the double mutation A366D/S367A decreased the affinity, but to a lesser extent (K_d being increased to 640 μM; Table 2). Analyzing the $g(V)$ curves and determining the A value suggested that the P-loop substitutions did not affect the closing transitions markedly (Table 2).

As shown in the schematic channel structure of Fig. 1B, the three residues involved in the largest modification of bupivacaine block (positions Thr372, Ile373 and Thr374) are located in the descending helix of the P-loop. Based on the generally accepted assumption of a close homology between the pore domain of Kv2.1 and KcsA, we conclude that the discussed residues are not in contact with the external solution. The decrease in binding affinity of the S5-S6 linker substituted chimera therefore seems associated with modifications of the bupivacaine binding to the internal vestibule site.

Discussion

A Working Hypothesis. To gain insights into the molecular mechanisms of anesthesia, we analyzed the effects of bupivacaine on a series of voltage-gated K^+ channels (Kv1.1, -1.2, -1.5, -2.1, -3.1, and -3.2) and various mutant channels derived from Kv2.1. Summarizing the main findings, we showed that 1) the block of Kv2.1 deviated from the block of the other channels and 2) introducing some Kv1.2 residues in Kv2.1 introduced Kv1.2 features, whereas introducing other Kv1.2 residues changed the blocking behavior in another direction; i.e., they drastically reduced the bupivacaine affinity.

Numerical simulations showed that the block could be described by a simple unitary state diagram (Scheme 2) in which the deviation of Kv2.1 is seen in the relatively high probability to pass into a bound closed state at depolarization. This means that in Kv2.1, the bupivacaine molecule is partly trapped in the internal vestibule of the channel at repolarization, whereas in the other channels, bupivacaine prevents the channel from closing.

This deviating feature of Kv2.1 is in line with the results from other studies, suggesting Kv2.1 to be selectively sensitive to certain pharmacological compounds, such as 4-aminopyridine and propafenone (Kirsch et al., 1993; Madeja et al., 2003).

Introducing Kv1.2 residues into positions 395 and 398 of Kv2.1 induced Kv1.2 features (i.e., decreased probability of closing), whereas substitutions of other S6 residues did not modify the bupivacaine block. Introducing Kv1.2 residues into positions 372, 373, and 374 of Kv2.1 decreased the bupivacaine affinity. The mutational effects on the Kv2.1 kinetics (Scheme 2) can be summarized as in Scheme 3.

The Mu372 mutation leads to modified binding of bupivacaine (quantitatively described by a decreased affinity, K_d), and Mu395 to modified closing of the channel in bound state (quantitatively described by the trapping factor A).

The residues substituted in Mu372 and in Mu395 are most probably not accessible for bupivacaine (but see Pascual et

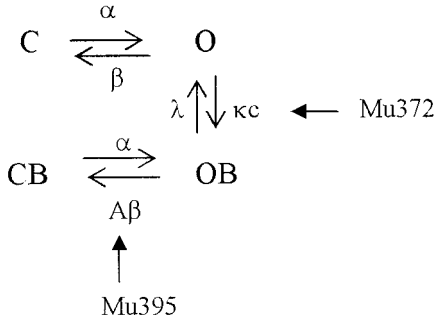

Scheme 3.

al., 1995). Both groups of residues are also located near each other. Homology simulations, in which Kv2.1 and chimeras were constructed on basis of the KcsA channel (see *Materials and Methods*), suggest that the distances between them range from 3.2 to 7.5 Å; the shortest distance is between S374 and C398 in the Mu372 channel (see Fig. 1A). An attractive idea is that the apparently different effects of these two groups of mutations with reference to the blocking behavior are caused by a similar mechanism. The following working hypothesis suggests such a unitary mechanism.

We assume that bupivacaine in wild-type Kv2.1 is bound inside the internal vestibule and thereby blocks the K^+ permeation through the channel. We also assume that bupivacaine has full access to its internal vestibule binding sites in open wild-type Kv2.1 channels. Mutation G395S/C398A is assumed to modify the open conformation (possibly by decreasing the entrance diameter, impairing the entrance of bupivacaine into the vestibule), causing bupivacaine to bind to a blocking site in the internal mouth region rather than to its site in the internal vestibule, thereby preventing channel closing. Mutation T372V/I373V/T374S is assumed to modify the open conformation even more (possibly by further decreasing the diameter), blocking the access of bupivacaine to any blocking site.

Related Findings in Other Studies. Binding of local anesthetics to an open-state dependent site in an internal vestibule was postulated early (Hille, 1977), as was the binding of other channel blocking compounds (Armstrong, 1971; Kristbjarnarson and Århem, 1982). Molecular studies later confirmed these early suggestions (Ragsdale et al., 1994; Yellen et al., 1991; Choi et al., 1993; Kirsch et al., 1993; for another view, see del Camino et al., 2000), most recently by using crystallographic methods (Zhou et al., 2001; Jiang et al., 2002).

The fact that point mutations in the N-terminal end of S6 (Mu395) modify the blocking kinetics so drastically (from trapping to nontrapping) is remarkable, in view of the distance between the substituted residues (395 and 398) and the assumed gating region, the S6 bundle crossing. However, some recent findings may make our working hypothesis less far-fetched. One is that a more closely located glycine (G401) may be the critical hinge for the gating mechanism (Jiang et al., 2002; Yifrach and MacKinnon, 2002). Another is that the I470C mutation in Shaker (corresponding to I405 in Kv2.1) induces trapping of TEA and C_{10} (Holmgren et al., 1997). Yet another finding is that V373 in Kv2.1 affects the TEA binding, possibly without being part of the binding site (Kirsch et al., 1992).

Physical Nature of the Bupivacaine Binding. The exact location and the physical nature of the site(s) and bond(s) between channel and bupivacaine are unknown. The S6 segment has been reported to form part of the binding site/sites of local anesthetics (Ragsdale et al., 1994), of longer quaternary ammonium ions (Choi et al., 1993) and of 4-aminopyridine (Kirsch et al., 1993), whereas the P-loop has been reported to be involved in tetraethyl ammonium binding (Yellen et al., 1991; Choi et al., 1993). The residues of the S6 segment reported to be critical for local anesthetic binding in Na^+ channels are aromatic (Ragsdale et al., 1994). Likewise, the residues critical for antiarrhythmic binding in HERG channels have been reported to be aromatic (Mitcheson et al., 2000). Both studies suggest that local anesthetics and antiarrhythmic drugs form ion-dipole and dipole-dipole π bonds with the channel. As seen in Fig. 1, no aromatic residues are present in the S6 segment of the channels studied, excluding the possibility of forming ion-dipole π bonds and reducing the possibility of forming dipole-dipole π bonds for the bupivacaine molecule in the internal vestibule. Thus, we have to search for other types of interactions between bupivacaine and the K^+ channels studied. Thermodynamic considerations of our data on Kv2.1 suggest that they are hydrophobic. The temperature experiments allow us to calculate the binding energy (as enthalpy ΔH) from the van't Hoff relation

$$\Delta H = R \ln[K_d(T_1)/K_d(T_2)]T_1T_2/(T_2 - T_1) \quad (6)$$

where R is the gas constant, $K_d(T_1)$ and $K_d(T_2)$ are dissociation constants at temperatures T_1 = 297 K and T_2 = 305 K. Calculations based on the experimental estimations listed in Table 3 yielded a ΔH value of 20.8 kJ/mol, which is within the range of hydrophobic bond energies encountered in biological processes (Freifelder, 1985). The associated entropy value ΔS is calculated from the equation

$$\Delta S = (\Delta H - \Delta G)/T \quad (7)$$

where ΔS is the entropy change and ΔG is the Gibb's energy, given by

$$\Delta G = -RT \ln(1/K_d) \quad (8)$$

with molar K_d, was 19.8 kJ/mol/K, and thus supported the hypothesis of hydrophobic bonds between bupivacaine and Kv2.1 (Cantor and Schimmel, 1980). Taking into account the fact that the dissociation constants for bupivacaine binding to channels expressed in oocytes may be artifactually too high (compare Lipka et al., 1998), the ΔS value would be even higher. This would further strengthen the hydrophobic bond hypothesis (see also Dickinson et al., 1993).

Most substitutions in the present investigation concern residues not directly constituting a part of the internal vestibule wall. Only residues 404 and 409 point in the direction of the cavity center. Substitutions of these residues, however, affected neither the bupivacaine binding nor the closing transition of the bupivacaine-bound channel, despite changes in hydrophobicity and size (Table 4). Thus, we suggest that bupivacaine mainly forms hydrophobic bonds with internal vestibule residues, not modified in the present investigation.

Concluding Remark. The fact that only Kv2.1 traps the bupivacaine molecule is remarkable, considering the close structural relationship within the Kv family. Even more remarkable is the fact that this ability can be related to one/two amino acids, as is also the fact that the bupivacaine affinity can be drastically reduced by substitutions of a few residues that do not constitute a part of the binding site. Similar differences concerning pharmacological action are likely to be

TABLE 3
Thermodynamic values for the binding of bupivacaine to Kv2.1 at +60 mV
Dissociation constants at different temperatures. Each value represents three to six measurements.

K_d			
297 K	305 K	Enthalpy ΔH	Entropy ΔS
		kJ/mol	*kJ/mol/K*
220 ± 30	180 ± 20	18.9	20.8

TABLE 4

Changes in hydrophobicity and size for the mutated channels

Hydrophobicity values given as difference between hydropathy indices for substituted residue and wild-type residue (Kyte and Doolittle, 1982). Positive values imply increased hydrophobicity. Size change given as change in residue volume, calculated from densitometric measurements (Zamyatnin, 1972).

Channel	Substitutions	Hydrophobicity Change	Size Change
S6 Mutations			
Mu395	G395S	−0.4	+48
	C398A	−0.7	−18
Mu404	V404T	−4.9	−17
Mu409	I409V	−0.3	−16
	I411V	−0.3	−16
	N414S	+4.3	−24
Mu417	S417N	−2.7	+32
	E418Y	+2.2	+40
P-loop Mutations			
Mu366	A366D	−5.3	+25
	S367A	+2.6	−12
Mu372	T372V	+4.9	+20
	I373V	−0.3	−16
	T374S	−0.1	−23
Mu383	I383M	−2.6	−2
	Y384V	+5.5	−18

found within the same subtype when comparing different species. This highlights the importance of investigating relevant channel subtypes when analyzing pharmacological effects, especially when extending a pharmacological study of an animal system to humans.

Appendix

Alternative Blocking Schemes for Kv2.1. The result of the fitting procedure above showed that the block of the Kv2.1 channel could successfully be explained by Scheme 2. A number of other blocking schemes were also tested, but no scheme could equally well explain the totality of the experimental data. Scheme 4 explained the experimental $I(t)$ and $g(V)$ curves at room temperature, but not corresponding curves at 34°C.

Fitting this scheme to the experimental data in Fig. 5A gave a dissociation constant (at 0 mV) for the open-state–dependent binding (K_{d1}) of 620 μM and one for the state-independent binding (K_{d2}) of 710 μM. The mean values of K_{d1} and K_{d2} were 530 ± 80 and 660 ± 70 μM, respectively.

However, this scheme could not be used to successfully describe the temperature effect. Using the blocking rate constants obtained from fitting Scheme 4 to the experimental curves at 24°C, it was not possible to predict the experimental time course at 32°C (which showed, for instance, no peak at +60 mV). Similarly, it was not possible to use Scheme 4 to explain the experimental time courses at +100 mV. Together with the finding that Kv2.1 does not have external binding sites, these facts make Scheme 4 unlikely as an explanation of the bupivacaine effect on Kv2.1.

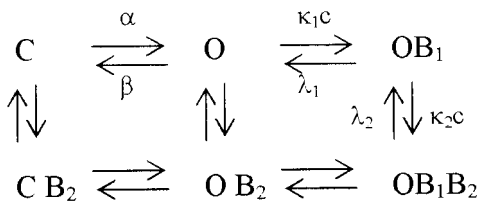

Scheme 4. Combination of open-state–dependent (B_1) and state-independent (B_2) mechanisms.

Acknowledgments

We are grateful to Alexandra Zirpins for skillful technical assistance, to Dirk Isbrandt, Thorsten Leicher, and Olaf Pongs (Center of Molecular Neurobiology, University of Hamburg) for cRNA of the wild-type and mutated channels, and to Lars-Inge Olsson (Astra Pain Control) for local anesthetic substances and for pharmacological insights. We also would like to thank Fredrik Elinder and Peter Larsson for constructive discussions on different versions of the manuscript, Clas Blomberg (Department of Theoretical Physics, Royal Institute of Technology, Stockholm) for mathematical assistance, and John-Patrik Berlips, Göran Klement, and Roope Männikö for help with computer work.

References

Albright G (1979) Cardiac arrest following regional anesthesia with etidocaine or bupivacaine. *Anesthesiology* **51:**285–287.

Åqvist J and Luzhkov V (2000) Ion permeation mechanism of the potassium channel. *Nature (Lond)* **404:**881–8844.

Armstrong CM (1971) Inactivation of tetraethylammonium ion derivatives with the potassium channels of giant axons. *J Gen Physiol* **58:**413–437.

Butterworth IVJF and Strichartz GR (1990) Molecular mechanisms of local anesthesia: a review. *Anesthesiology* **4:**711–734.

del Camino D, Holmgren M, Liu Y, and Yellen G (2000) Blocker protection in the pore of a voltage-gated K^+ channel and its structural implications. *Nature (Lond)* **404:**321–325.

Cantor CR and Schimmel PR (1980) The conformation of biological macromolecules, in *Biophysical Chemistry, Part 1*, pp 287–288, WH Freeman and Company, San Francisco.

Choi KL, Mossman C, Aube J, and Yellen G (1993) The internal quaternary ammonium receptor site of Shaker potassium channels. *Neuron* **10:**533–541.

Dickinson R, Franks NP, and Lieb WR (1993) Thermodynamics of anesthetic/protein interactions. Temperature studies on firefly luciferase. *Biophys J* **64:**1264–1271.

Doyle DA, Cabral JM, Pfuetzner RA, Kuo A, Gulbis JM, Cohen SL, Chait BT, and MacKinnon R (1998) The structure of the potassium channel: molecular basis of K^+ conduction and selectivity. *Science (Wash DC)* **280:**69–77.

Elinder F, Madeja M, and Arhem P (1996) Surface Charges of K channels. Effects of strontium on five cloned channels expressed in *Xenopus oocytes*. *J Gen Physiol* **108:**325–332.

Finkel AS and Gage PW (1985) Conventional voltage clamping with two intracellular microelectrodes, in *Voltage and Patch Clamping with Microelectrodes* (Smith T Jr, et al., eds), pp 47–93, American Physiological Society, Baltimore.

Franqueza L, Longobardo M, Vicente J, Delpon E, Tamkun MM, Tamargo J, Snyders DJ, and Valenzuela C (1997) Molecular determinants of stereoselective bupivacaine block of hKv1.5 channels. *Circ Res* **81:**1053–1064.

Freifelder D (1985) *Principles of Physical Chemistry with Applications to the Biological Sciences.* 2nd ed. Jones and Bartlett, Boston.

Harris T, Shahidullah M, Ellingson JS, and Covarrubias M (2000) General anesthetic action at an internal protein site involving the S4–S5 cytoplasmic loop of a neuronal K^+ channel. *J Biol Chem* **275:**4928–4936.

Hille B (1977) Local anesthetics: hydrophilic and hydrophobic pathways for the drug-receptor reaction. *J Gen Physiol* **69:**497–575.

Hille B (2001) *Ionic Channels of Excitable Membranes.* Sinauer Associates, Inc, Sunderland, MA.

Holmgren M, Smith PL, and Yellen G (1997) Trapping of organic blockers by closing of voltage-dependent K^+ channels: evidence for a trap door mechanism of activation gating. *J Gen Physiol* **109:**527–535.

Hondeghem LM and Katzung BC (1977) Time and voltage dependent interactions of antiarrhythmic drugs with cardiac sodium channels. *Biochim Biophys Acta* **472:** 373–398.

Jiang Y, Lee A, Chen J, Cadene M, Chait BT, and MacKinnon R (2002) The open pore conformation of potassium channels. *Nature (Lond)* **417:**523–526.

Kirsch GE, Drewe JA, Hartmann HA, Taglialatela M, de Biasi M, Brown AM, and Joho RH (1992) Differences between the deep pores of K^+ channels determined by an interacting pair of nonpolar amino acids. *Neuron* **8:**499–505.

Kirsch GE, Shieh CC, Drewe JA, Vener DF, and Brown AM (1993) Segmental exchanges define 4-amonopyridine binding and the inner mouth of K^+ pores. *Neuron* **11:**503–512.

Kristbjarnarson H and Århem P (1982) The effect of crown ethers on ionic currents in myelinated nerve fibres from *Xenopus laevis*. *Acta Physiol Scand* **123:**261–268.

Kyte J and Doolittle RF (1982) A simple method for displaying the hydrophobic character of a protein. *J Membr Biol* **157:**105–132.

Lipka LJ, Jiang M, and Tseng G (1998) Differential effects of bupivacaine on cardiac K channels: role of channel inactivation and subunit composition in drug channel interaction. *J Cardiovasc Electrophysiol* **9:**727–742.

Longobardo M, Gonzalez T, Navarro-Polanco R, Caballero R, Delpon E, Tamargo J, Snyders DJ, Tamkun MM, and Valenzuela C (2000) Effects of a quaternary bupivacaine derivative on delayed rectifier K^+ currents. *Br J Pharmacol* **130:**391–401.

Madeja M, Musshoff U, and Speckmann EJ (1991) A concentration-clamp system allowing two-electrode voltage-clamp investigations in oocytes of *Xenopus laevis*. *J Neurosci Methods* **38:**267–269.

Madeja M, Leicher T, Friederich P, Punte MA, Haverkamp W, Musshoff U, Breithardt G, and Speckmann EJ (2003) Molecular site of action of the antiarrhythmic drug propafenone at the voltage-operated potassium channel Kv2.1. *Mol Pharmacol* **63:**1–10.

Mather LE and Chang DH (2001) Cardiotoxicity with modern local anaesthetics: is there a safer choice? *Drugs* **61:**333–342.
Mitcheson JS, Chen J, Lin M, Culberson C, and Sanguinetti MC (2000) A structural basis for drug-induced long QT syndrome. *Proc Natl Acad Sci USA* **97:**12329–12333.
Pascual JM, Shieh CC, Kirsch GE, and Brown AM (1995) K^+ pore structure revealed by reporter cysteines at inner and outer surfaces. *Neuron* **14:**1055–1063.
Ragsdale DS, McPhee JC, Scheuer T, and Catterall WA (1994) Molecular determinants of state-dependent block of Na^+ channels by local anesthetics. *Science (Wash DC)* **265:**1724–1728.
Scholle A, Koopmann T, Ludwig J, Pongs O, and Benndorf K (2000) Structural elements determining activation kinetics in Kv2.1. *Recept Channels* **7:**65–75.
Stühmer W, Stocker M, Sakman B, Seeburg P, Baumann A, Grupe A, and Pongs O (1988) Potassium channels expressed from rat brain cDNA have delayed rectifier properties. *FEBS Lett* **242:**199–206.
Valenzuela C, Delpon E, Tamkun MM, Tamargo J, and Snyders DJ (1995) Stereoselective block of a human cardiac potassium channel (Kv1.5) by bupivacaine enantiomers. *Biophys J* **69:**418–427.
Yellen G (1998) The moving parts of voltage-gated ion channels. *Q Rev Biophys* **31:**239–395.
Yellen G, Jurman ME, Abramson T, and MacKinnon R (1991) Mutations affecting internal TEA blockade identify the probable pore-forming region of a K^+ channel. *Science (Wash DC)* **251:**939–942.
Yifrach O and MacKinnon R (2002) Energetics of pore opening in a voltage-gated K^+ channel. *Cell* **111:**231–239.
Zamyatnin AA (1972) Protein volume in solution. *Prog Biophys Mol Biol* **24:**107–123.
Zhou M, Morais-Cabral JH, Mann S, and MacKinnon R (2001) Potassium channel receptor site for the inactivation gate and quaternary amine inhibitors. *Nature (Lond)* **411:**657–661.

Address correspondence to: Peter Århem, The Nobel Institute for Neurophysiology, Department of Neuroscience, Karolinska Institutet, SE-171 77 Stockholm, Sweden. E-mail: peter.arhem@neuro.ki.se